

MECHANICAL AND TEMPERATURE CONTACT IN FUEL ROD CLADDING

B. E. FREDRIKSSON, S. G. RYDHOLM

*Department of Mechanical Engineering, Linköping Institute of Technology,
S-581 83 Linköping, Sweden*

SUMMARY

Due to temperature rise the fuel element pellets get into mechanical contact with the cladding and will together with the gas pressure cause high stress states. Existing cracks and particles between fuel and cladding may further increase the stresses. Due to irregularities there may be a welding between the fuel and cladding and a following temperature decrease will cause tensile stresses which may initiate cracks. In order to do a safe design of the fuel cladding assembly it is worthwhile to be able to analyse these phenomena.

For the mechanical contact between fuel and cladding a slip criterion relating contact shear stresses to the slip between fuel and cladding is introduced. Because of irreversibility an incremental formulation is made. With this slip criterion with associated slip rule it is possible to simulate different types of frictional behaviour of the fuel cladding interface. It is also possible to allow for eventual welding between fuel and cladding. That is, cohesive stresses are allowed for at the assumed welding positions. The incremental governing equations are solved by means of the finite element method. In the computer program developed a Coulomb type of slip criterion with associated ideal or hardening slip rule is included. In the ideal model the coefficient of friction is constant and in the hardening model the coefficient of friction depends on the slip.

The transient temperature problem is also solved by means of the finite element method. The method proposed by Miya, Hashimoto and Ando (SMiRT-3 paper C3/8) of taking the eventual initial gap between fuel and cladding into account was adopted.

The paper presents results for the effect of different types of slip rules on the contact stress distribution. It is shown that the contact shear stress is smaller for the hardening model than for the ideal model. It is also shown that a crack in the fuel increases the contact stresses and that at temperature decrease high tensile stresses arise after eventual welding. It is also shown how particles between fuel and cladding influence the stresses. Also here the effect of eventual welding is studied. The present method is well suited to study cracks and crack propagation. The surfaces of the existing cracks are defined as contact surfaces and the crack extension work is calculated by releasing the nodes at the crack tip. As the crack surfaces are defined as contact surfaces eventual crack closure is automatically taken into account. Crack extension work is calculated for existing cracks in the cladding. It is shown that cracks in the fuel and particles between fuel and cladding will increase the crack extension work.

1. Introduction

The contact zone between fuel and cladding and cracks in fuel and cladding presents complex boundary conditions. Both mechanical and temperature contact problems are present. During the last decade mathematicians [1] have paid attention to the new type of boundary conditions that arise in mechanical contact problems. Panagiotopoulos [2] considers unilateral contact and friction boundary conditions. In this new type of boundary conditions inequalities are present. Thus, the variations appearing in the principle of virtual work are unilateral constituting a variational inequality. Panagiotopoulos proves the theorem of minimum potential energy with the inequality constraints, which constitutes a nonlinear programming problem. Variational inequalities are also discussed by Kalker [3]. The nonlinear programming problem are for practical problems (many degrees of freedom) time consuming and thus expensive. In the present paper some simplifying assumptions are made. In order to follow the loading history an incremental formulation is used. Within each increment it is assumed that the surface of contact is a priori known or it is known whether it is increasing or decreasing. Thus the boundary condition is bilateral. As a contact constitutive relation is a relation between the contact stress increment vector and the slip increment vector in the contact surface, a slip criterion with associated slip rule is used. This slip criterion and slip rule is analogous to the yield criterion and the flow rule in the theory of plasticity. By introducing the simplifying assumptions the problem is a variational equality problem and the nonlinearities could be treated in the usual way of structural mechanics [4].

The temperature contact problem is complex because there may be a gap between fuel and cladding which during loading cycles close causing changes in the properties of heat conduction. The conditions at the interface are accounted for by introducing a boundary element which couples the field of the fuel and that of the cladding. Both the temperature and the stress analysis are solved by means of the finite element method.

2. The Mechanical Contact

Consider two bodies A and B in contact. The problem is studied in the global three-dimensional cartesian coordinate system x_1, x_2, x_3 . At the contact surface Ω_c the local cartesian coordinate system η_1, η_2, η_3 is defined in the following way: The coordinate system is fixed to body B. $\eta_1\eta_2$ -plane is the tangential plane and η_3 is defined by the outward normal vector from body B to body A at the contact point studied. The bodies are bounded by the surfaces Ω^A and Ω^B and occupy the volumes V^A and V^B respectively. They are assumed to be loaded with surface loads $q_i(x_1, x_2, x_3)$ on Ω_q , volume loads $X_i(x_1, x_2, x_3)$, temperature loads $T(x_1, x_2, x_3)$ and heat sources $Q(x_1, x_2, x_3)$ in V . On Ω_u the displacements are assumed to be given and on Ω_c the bodies are in contact. It is to be observed that Ω_c varies with the load, $\Omega_c = \Omega_c(q_i, X_i)$. The displacements and strains are assumed to be small.

2.1 Contact Constitutive Equations

In most investigations dealing with contact problems including friction, a macroscopic type of Coulomb friction is assumed. It has been shown experimentally however ([5], [6]) that microslip occurs for tangential loads smaller than the frictional force as determined by the macroscopic coefficient of friction. From the experimental results it is clear that

the coefficient of friction increases with increasing slip. It is also demonstrated by the experiments that part of the slip is reversible and part is irreversible. In order to obtain a tool for studying the effects of the frictional properties of the contact surface, a contact constitutive relation is proposed. This relation consists of a general kind of slip criterion with associated slip rule. Due to the irreversible character of the friction phenomena an incremental formulation is made.

Consider the cartesian coordinate system η_1, η_2, η_3 at a contact point given on Ω_c . The contact stress increment vector is written

$$dp_i = (dp_1, dp_2, dp_3) \text{ on } \Omega_c \quad (1)$$

In the following, when the indices $\alpha, \beta, \gamma, \delta$ occur, they are assumed to range from 1 to 2 and refer to the local coordinate system η_1, η_2, η_3 . A detailed derivation of the slip rule is given by Fredriksson [7]. The derivation of the slip rule is based upon two *basic assumptions*

1. The slip increment dv_α is linearly dependent on the contact stress increment. That is,

$$dv_\alpha = du_\alpha^A - du_\alpha^B = h_{\alpha\beta} dp_\beta \quad (2)$$

2. It exists a *slip surface* $g(p_i) = 0$ in the contact stress space on which slip will occur. At each state of the slip no further slip will occur unless

$$\frac{\partial g}{\partial p_i} dp_i > 0 \quad (3)$$

The first assumption implies that the slip has the same direction as the outward normal vector to the locus generated from the intersection between the surface and the plane $p_3 = \text{constant}$.

For *slip hardening* we obtain

$$dv_\alpha = \frac{1}{L} \frac{(\partial g / \partial p_\alpha)(\partial g / \partial p_\beta)}{(\partial g / \partial p_\delta)(\partial g / \partial p_\delta)} dp_\beta \text{ on } \Omega_c^S \quad (4)$$

when $g = 0$, $\frac{\partial g}{\partial p_i} dp_i > 0$, $p_3 < 0$.

Ω_c^S is the part of Ω_c , where the slip criterion is satisfied. In the part Ω_c^a of Ω_c where the slip criterion is not satisfied there is no slip increment and the displacement increment must satisfy

$$dv_\alpha = du_\alpha^A - du_\alpha^B = 0 \text{ on } \Omega_c^a \quad (5)$$

If we assume *ideal slip* eq. (4) is replaced by the slip rule

$$dv_\alpha = \lambda \frac{\partial g}{\partial p_\alpha} \text{ on } \Omega_c^S \quad (6)$$

$\lambda \geq 0$ when $g = 0$ and $\frac{\partial g}{\partial p_i} dp_i = 0$, $p_3 < 0$

$\lambda = 0$ when $g < 0$ or, $\frac{\partial g}{\partial p_i} dp_i < 0$, $p_3 < 0$

$\frac{\partial g}{\partial p_i} dp_i > 0$ does not exist in ideal slip. In ideal slip the slip surface is fixed.

The functions g and L depend on properties of the contact surface, for instance type of material, surface roughness and manufacturing process. In the case of ideal slip the parameter λ is indeterminate.

Assuming *Coulomb isotropic slip criterion* we obtain

$$g(p_i) = \frac{1}{\mu} (p_\alpha p_\alpha)^{1/2} + p_3, \quad p_3 < 0 \quad (7)$$

and the associated slip rule

$$dv_\alpha = \frac{1}{L} \frac{p_\alpha p_\beta}{p_\delta p_\delta} dp_\beta \quad (8)$$

μ is the coefficient of friction.

It is easy to show [4] that the function L , which can be called the *slip modulus* could be written

$$L = - p_3 \frac{d\mu(v_e)}{dv_e} \quad (9)$$

v_e is the *effective slip* [4].

Thus, from the single curve $\mu = \mu(v_e)$ the slip modulus is obtained. Such curves have been published elsewhere [6].

The slip hardening rule used is

$$\mu/\mu_m = 1 - (1 - \beta) \exp(-nv_e) \quad (10)$$

μ_m is the maximum coefficient of friction, β defines the initial coefficient of friction and n defines the degree of hardening.

2.2 Crack Closure Problems

The present method is applicable to fracture mechanics problems as well. In terms of crack extension work the stress intensity factors may be calculated both for opening and closing cracks.

In terms of stress intensity factors the crack extension work is written (coplanar extension).

$$C = \frac{\kappa+1}{8G} (K_I^2 + K_{II}^2) + \frac{1}{2G} K_{III}^2 \quad (11)$$

K_I , K_{II} , K_{III} are the stress intensity factors in mode I, II and III respectively. $\kappa = 3-4\nu$ plane deformation, $\kappa = (3-\nu)/(1+\nu)$ plane stress and $G = E/2(1+\nu)$. E is the modulus of elasticity and ν is Poissons ratio.

Assume a virtual quasistatic crack growth from a state a with fracture area S to a state b with fracture area $S + \Delta S$. This gives rise to a new crack surface Ω_{cr}^+ . The work done on the fracture process zone between stages a and b per unit of fracture area is the crack extension work

$$C = - \lim_{\Delta S \rightarrow 0} \frac{1}{\Delta S} \int_{\Omega_{cr}} \int_a^b p_i du_i d\Omega \quad (12)$$

p_i is the traction acting on the fracture process zone and u_i is the displacement.

As proposed by Hellan [8] the finite element method seems to be a useful tool to calculate the crack extension work. The nodal point forces at the crack tip are calculated. These forces are then relaxed to zero and the work done by the forces are calculated. In nonlinear problems (for instance crack closure problems) the relaxation must be performed incrementally. The present method is well suited for this process and can also handle crack closure problems. Nodal points on an existing crack are defined as contact nodes. During loading or unloading the cracked surfaces will be checked for eventual closure. When at the crack tip positive contact forces arise the contact nodes are released and the work done by the contact forces during relaxation is calculated. By defining contact node-pairs in several directions at the crack tip the present method can be used to calculate the crack extension work in several directions and the direction of crack propagation may be predicted.

When the crack is closing and shear stresses develop at the contact energy is dissipating due to friction. The energy dissipated during the virtual crack extension is written [7]

$$W^S = \lim_{\Delta S \rightarrow 0} \frac{1}{\Delta S} \int_{\Omega_c} \int_1^2 p_\alpha dv_\alpha d\Omega \quad (13)$$

Thus, the sum of C and W^S expresses the total energy dissipated.

2.3 The Finite Element Solution

The theory presented have been included in a finite element computer program for plane stress, plane strain and axisymmetric problems. Coulomb slip criterion with associated ideal and hardening slip rule has been used. The subroutines handling the contact nonlinearities have been written as to be applicable to any finite element computer program. The routine handling the nonlinearities needs the stiffness matrix transformed to local coordinates at contact nodes. For details concerning the finite element formulation the reader are referred to Fredriksson [4], [7].

3 The Temperature Contact

The partial differential equation for heat conduction is written

$$\frac{\partial}{\partial x} (\lambda_x \frac{\partial T}{\partial x}) + \frac{\partial}{\partial y} (\lambda_y \frac{\partial T}{\partial y}) + \frac{\partial}{\partial z} (\lambda_z \frac{\partial T}{\partial z}) + Q - \rho c_p \frac{\partial T}{\partial t} = 0 \quad (14)$$

T = temperature

t = time

ρ = density

$\lambda_x, \lambda_y, \lambda_z$ = thermal conductivities

Q = thermal source

c_p = specific heat

The finite element formulation utilizes the equivalence of minimizing the functional

$$\chi = \int_V \left\{ \frac{1}{2} [\lambda_x \left(\frac{\partial T}{\partial x}\right)^2 + \lambda_y \left(\frac{\partial T}{\partial y}\right)^2 + \lambda_z \left(\frac{\partial T}{\partial z}\right)^2] - [Q - \rho c_p \frac{\partial T}{\partial t}] T \right\} dV + \int_{\Omega} \left[q + \frac{1}{2} \alpha T \right] T d\Omega \quad (15)$$

α = heat transfer coefficient

q = flow

Introducing shape functions N_i the temperature is written

$$T = \sum N_i T_i \quad (16)$$

By dividing the body into finite elements, calculating the functional χ^e for each element and summing the contributions a time dependent system of algebraic equations are obtained

$$KT + c \frac{\partial T}{\partial t} - Q_T = 0 \quad (17)$$

$$K = H + A$$

The conductivity matrix H is

$$h_{ij} = \sum_e \int_V \lambda_x \frac{\partial N_j}{\partial x} \frac{\partial N_i}{\partial x} + \lambda_y \frac{\partial N_j}{\partial y} \frac{\partial N_i}{\partial y} + \lambda_z \frac{\partial N_j}{\partial z} \frac{\partial N_i}{\partial z} dV \quad (18)$$

The heat transfer matrix A is

$$a_{ij} = \sum_e \int_{\Omega_e} \alpha N_i N_j d\Omega \quad (19)$$

The capacity matrix c is

$$c_{ij} = \sum_e \int_V \rho c_p N_i N_j dV \quad (20)$$

The flow Q_T is

$$Q_{T_i} = Q_i - \sum_e \int_{\Omega_e} (q N_i + \alpha N_i (\sum_j \Delta T_j)) d\Omega \quad (21)$$

where $\Delta T_j = T_j - T_j^*$, T_j^* = surrounding temperature

If in the present problem a functional χ^A for the fuel and a functional χ^B for the cladding is considered the resulting systems of equations must be coupled according to the contact condition at the interface. If there is a mechanical contact with pressure the temperature solution could be obtained directly by using the appropriate thermal conductivity. A total functional for both the fuel and the cladding results in the standard system of equations to solve. If, however, there is a gap between fuel and cladding the situation is, as pointed out by Miya, Hashimoto and Ando [9], more complex. Consider a two-dimensional problem with triangular finite elements with linear shape functions. The local coordinate at the interface is η_1 (Fig. 1). The temperatures at the interfacial nodes

k, l and k', l' are indicated T_k, T_l and $T_{k'}, T_{l'}$, respectively. Assuming a linear temperature distribution in the interfacial region

$$\begin{aligned} T^A &= T_k + \frac{\eta_1}{L} (T_l - T_k) \\ T^B &= T_{k'} + \frac{\eta_1}{L} (T_{l'} - T_{k'}) \end{aligned} \quad (22)$$

By minimizing the functionals χ^A and χ^B we obtain after integration between nodes k, l and k', l' respectively.

$$\begin{bmatrix} (\partial \chi^A / \partial T_k)_{kl} \\ (\partial \chi^A / \partial T_l)_{kl} \\ (\partial \chi^B / \partial T_{k'})_{k'l'} \\ (\partial \chi^B / \partial T_{l'})_{k'l'} \end{bmatrix} = \frac{\alpha L}{6} \begin{bmatrix} 2 & 1 & -2 & -1 \\ 1 & 2 & -1 & -1 \\ -2 & -1 & 2 & 1 \\ -1 & -2 & 1 & 2 \end{bmatrix} \begin{bmatrix} T_k \\ T_l \\ T_{k'} \\ T_{l'} \end{bmatrix} \quad (23)$$

Eq. (23) expresses the contribution to the heat transfer matrix in eq. (19). Thus, the effect of the heat transfer at the interface could be taken into account by introducing a boundary element with a heat transfer matrix as eq. (23).

4 Numerical Example

4.1 The Problem Studied

The fuel element of Fig. 2 was studied. It was assumed that there exist ten cracks in fuel and cladding. The cracks in the cladding are assumed to coincide with those of the fuel. This assumption was made in order to reduce the size of the problem. Thus, a segment of 18 degrees was studied. In the temperature calculations the influence of existing cracks was not taken into account. For the stress analysis elastic plane strain conditions were assumed. The material properties in the fuel and the cladding were obtained from Karlsson [10] and Malén [11]. Temperature variation of the modulus of elasticity was accounted for.

In the finite element model triangular elements with linear displacement and temperature fields were used. In the analysis model 300 elements and 400 degrees of freedom were used.

4.2 The Temperature Field

In the temperature calculation a uniform heat generation of 50 kW/m was assumed. The cooling water temperature was set to 286°C. From Fig. 3 which shows the normalized temperature distribution for stationary conditions it is clear that the temperature drop between the fuel and the cladding is as expected much larger than in the cases of contact without or with pressure. The transient temperature distribution for the case with gap between fuel and cladding is shown in Fig. 4. It is seen how the temperature in the fuel is increasing with time while the temperature in the cladding is not increased very much. This result is opposite to the results obtained by Miya, Hashimoto and Ando [9] in the finite element calculations for fast reactors. This is of course explained by the fact that they used coolant of air while we used water. It should be pointed out that we used a constant

heat generation which gives a much faster temperature rise than in the real in pile case. The finite element computer program used in this calculations was the FEMTEMP II [12] program. The material properties were assumed independent of temperature.

4.3 Stress Analysis

The stress analysis was performed for the case when there was initial contact between fuel and cladding at a power generation of 40 kW/m. The power generation was then increased to 56 kW/m and the contact stresses etc were calculated. Results are presented for the stationary case.

Fig. 5 shows the normalized normal contact stress distribution p_3 (pressure is defined negative) for different coefficients of friction. p_0 is the uniform contact pressure obtained when there are no cracks present. Due to the cracks present in both fuel and cladding the contact stress is very much increased near the crack. The cladding is due to the cracks softer which explain that $-p_3/p_0 < 1$ far from the crack. The contact stress is larger for larger coefficients of friction. This is explained by the fact that a larger coefficient of friction will increase the tangential stiffness of the cracked cladding. Fig. 6 shows the contact shear stress distribution for three types of slip rules. Both the ideal models with $\mu = 0.1$ and $\mu = 0.2$ results in greater shear stresses than the hardening model with initial coefficient of friction 0.02 and maximum coefficient of friction 0.2. It should be mentioned that slip takes place all over the interface except in a region near the symmetry line at 18° .

Calculations were next performed for the case of a particle between fuel and cladding at $\phi = 9^\circ$. In all cases (particle thicknesses from 0.05 mm to 0.2 mm) very high contact stresses were obtained at the position of the particle and the contact was lost elsewhere. This situation will also arise when there are irregularities in the fuel or when the fuel is cracked due to earlier temperature changes so that some part of the fuel is tilted causing concentrated contacts. At these very high pressures there may be a situation for "cold"-welding to the cladding. At a later temperature decrease high tensile stresses arise and will eventually initiate cracks in cladding and/or fuel. Fig. 7 shows results when welding followed by temperature decrease was assumed to have taken place.

Next the effect of different crack lengths in the cladding was studied. Fig. 8 shows that the normal contact stress far from the crack is decreasing with increasing crack length a . Although the gradients near the crack is influenced the normal contact stress is in all cases very high.

The crack extension work C for different crack length in the cladding was next studied. Also the effect of friction was studied. Fig. 9 shows the crack extension work as a function of the crack length and for two different coefficients of friction. It is noted that the crack extension work is decreased at increasing friction. The ideal model was assumed in this study. Another interesting observation is made. The crack extension work is increasing with increasing crack length to a certain limit where it starts to decrease. This positive effect is explained by the fact that for increasing crack length the softening (Fig. 8) of the cladding will offset the increase in C . Fig. 10 shows the effect of a particle of thickness 0.05 mm placed at $\phi = 18^\circ$. The crack extension work is increased very much and the effect of decreasing C at large crack length is maintained. Internal cracks in cladding have been studied by for instance Chopra, Wu and Hofman [13] who prescribed the pressure

distribution on the cladding. They studied cracks of relative length up to 0.3. Because of the prescribed pressure they could not take into account the effect of softening of the cladding and the above described effect of decrease in C could not be accounted for. The particle of 0.05 mm was next moved towards the crack and the crack extension work for different positions was calculated. The crack length was in all cases constant. The result is shown in Fig. 11. In positions close to the crack the crack is closing due to the effect of the particle. C then increases rapidly followed by a decrease as the particle is moving away from the crack. The particle will in the main part of the region cause crack extension work that is greater than that without the particle. A similar effect was observed by Chopra, Wu and Hofman [13] who considered a concentrated load instead of inserting a particle between fuel and cladding.

5 Conclusions

The method presented has been shown to be a useful tool when studying the contact phenomena at the interface between fuel and cladding. It is possible to study effects of different types of frictional properties on the normal and shear contact stress distribution. The method is also well suited for studying the influence of cracks in fuel and cladding. Stress intensity factors, or crack extension work for different types of cracks are easily calculated and eventual crack closures are automatically taken into account.

When studying the contact situation at fuel-cladding interface it is shown how the softening effect on the cladding due to increasing crack length influences the contact stress. It is also shown how this effect influences the crack extension work. For long cracks the crack extension work starts to decrease due to this softening effect. It is also shown that a particle between the fuel and cladding greatly influences the crack extension work. Except in a narrow region near the crack, the crack extension work is increased. High contact stresses are developed at the position of the particle. These high stresses may perhaps initiate cracks. The same effect is obtained if there are small irregularities in the fuel. The very high stresses at the interface may eventually cause cold welding or wedging to the cladding. A temperature decrease will immediately cause high tensile stresses and the fuel material which could not stand tensile stresses will be fractured. In the temperature calculations it is shown how different contact situations influences the temperature distribution. Another interesting effect that could be studied with the present method is the influence of the cracks in the fuel on the temperature distribution.

In the present study a very symmetrical situation has been analysed. It is, however, believed that the effects observed could be qualitatively transferred to a unsymmetrical situation. Although, the method of taking contact conditions into account is applied to elastic material assumptions the significance of the phenomena observed are believed to be valid. Of course the high stresses observed near the cracks and at the crack tips will cause yielding. Also some creep is probably present. It should be mentioned that the present contact model is coded as to be applicable to existing finite element programs and it is possible to include it in a program, which takes plasticity effects into account.

Acknowledgement

The authors are grateful to Messrs Axelsson, Fröier and Loyd for the possibility of using their finite element program for temperature calculations. Gratitude is also directed to Mr Jaroslav Mackerle for computer calculations and preparing figure drawings.

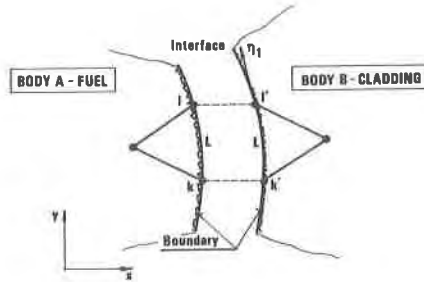


Fig. 1 Boundary elements in the temperature contact

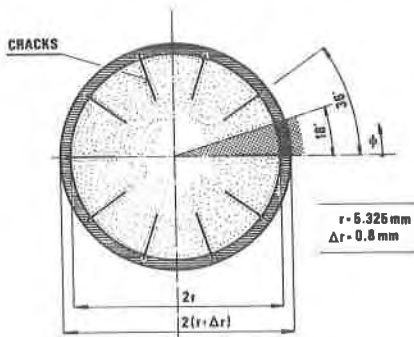


Fig. 2 Uraniumdioxide fuel with 10 radial cracks to a dept of $r/2$ and zircalloy cladding of thickness Δr with internal cracks to a (varying) dept a

References

- [1] DUVAUT, G., LIONS, J. L., Inequalities in mechanics and physics, Springer Verlag, New York, 1976.
- [2] PANAGIOTOPOULOS, P. D., A nonlinear programming approach to the unilateral contact and friction boundary value problem in the theory of elasticity. Ingenieur-Archiv 44, 1975, pp 421 - 432.
- [3] KALKER, J. J., Variational principles of contact elastostatics. Nov. 1975, Dept. of Mathematics, Delft University of Technology.
- [4] FREDRIKSSON, B., Finite element solution of surface nonlinearities in structural mechanics with special emphasis to contact and fracture mechanics problems. Comp. & Struct. 6, 1976, pp 281 - 290.
- [5] BOWDEN, F. P., TABOR, D., The friction and lubrication of solids. Oxford University Press, Vol. I (1958), Vol. II (1964).
- [6] LINDGREN, M., Drehmoment-Übertragung in Pressverbindungen, Konstruktion 25, 1973, 538 - 541.
- [7] FREDRIKSSON, B., On elastostatic contact problems with friction. A finite element analysis. Linköping Studies in Science and Technology, No. 6, 1976, Linköping, Sweden.
- [8] HELLAN, K., Energy considerations in static fracture mechanics. Publ. No. 73:6 Norwegian Inst. of Technology, Norway (1973).
- [9] MIYA, K., HASHIMOTO, M., ANDO, Y., Application of finite element method to thermal contact problems and experiments in fast reactor. Paper C3/8 in Proc. 3rd Int. Conf. on Struct. Mech. in Reactor Techn. 1975.
- [10] KARLSSON, B. G., Optimal rate of power increase in nuclear fuel. Dept. of Energy Conversion, Chalmers University of Technology, Gothenburg, Sweden 1976.
- [11] MALEN, K., Private communications, AB Atomenergi, Studsvik, Sweden.
- [12] AXELSSON, K., FRÖTIER, M., LOYD, D., FEMTEMP II, Chalmers University of Technology, Publ. No. 75:2, Dept. of Struct. Mech., 1975
- [13] CHOPRA, P. S., WU, T. S., HOFMAN, G. L., A fracture mechanics contribution to fuel element design and analysis. Paper C4/1 in Proc. 3rd Int. Conf. on Struct. Mech. in Reactor Techn., 1975.

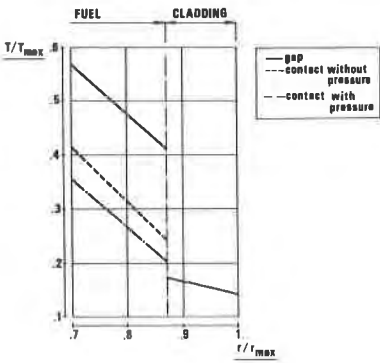


Fig. 3 Stationary temperature distribution T_i for different types of contact conditions

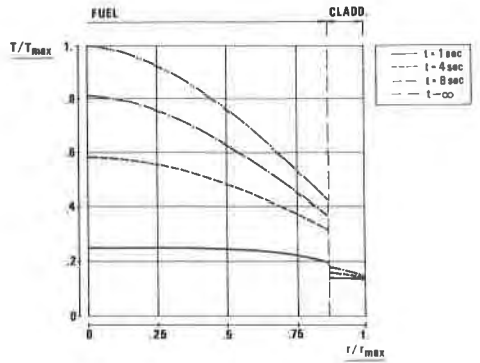


Fig. 4 Transient temperature distribution for gap between fuel and cladding

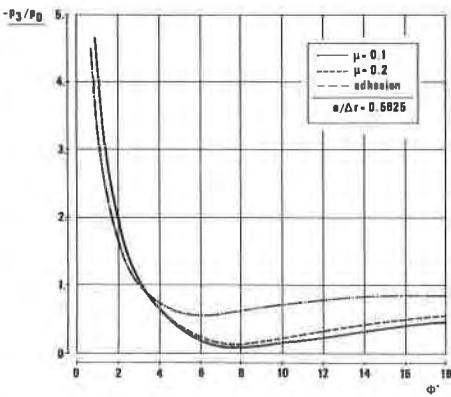


Fig. 5 Normalized normal contact stress for different coefficients of friction

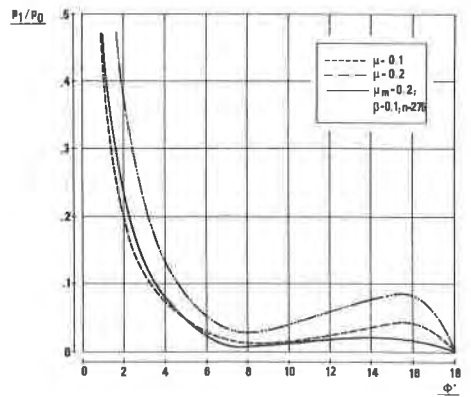


Fig. 6 Normalized contact shear stress for different type of slip models

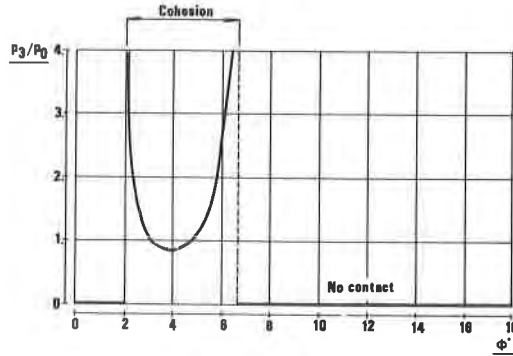


Fig. 7 Normal contact stress distribution for the case of assumed welding followed by temperature decrease. Complete cohesion is assumed

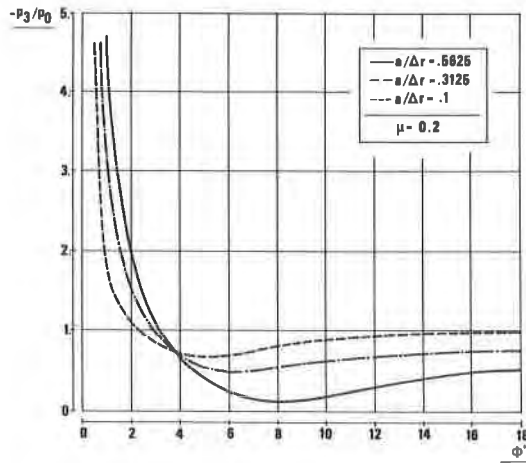


Fig. 8 Normal contact stress distribution for different crack length in the cladding

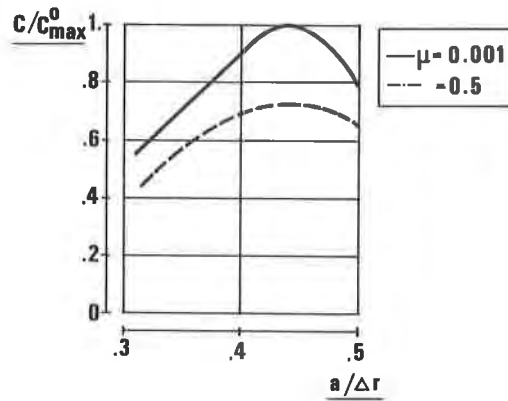


Fig. 9 The crack extension work C for different coefficients of friction as a function of crack length

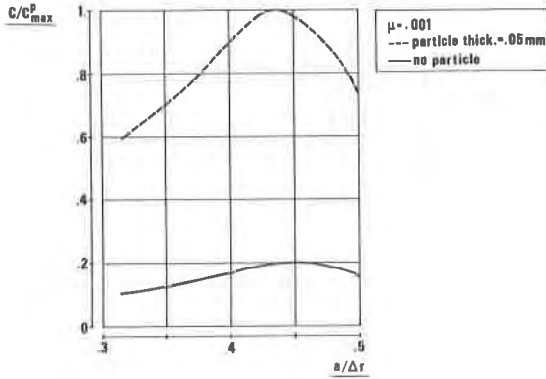


Fig. 10 The crack extension work as a function of crack length. The effect of a particle at the interface at a position $\phi = 18^\circ$.

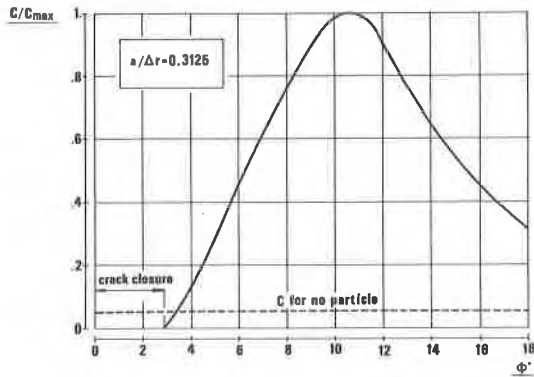


Fig. 11 The crack extension work C as a function of particle position ϕ between fuel and cladding